

# Fast-yet-accurate Variation-Aware Current and Voltage Modelling of Radiation-Induced Transient Fault

Hsuan-Ming (Ryan) Huang, Yuwen (Dave) Lin, and Charles H.-P. Wen

Department of Electrical and Computer Engineering, National Chiao Tung University, Hsinchu, Taiwan 300  
hmhuang.eed00g@g2.nctu.edu.tw, linyeuwen0112.eed04g@g2.nctu.edu.tw, opwen@g2.nctu.edu.tw

**Abstract**—For robust systems, it is important to mitigate radiation effect in early stages to reduce the design cost. Traditionally, a double-exponential current source is widely used to model the transient fault for analyzing the radiation effects. However, in light of complicating effects in the advanced technologies, such approach is no longer sufficient to estimate transient faults and may lead to inaccurate results. Therefore, we propose a fast-yet-accurate approach to model the radiation-induced transient fault, meanwhile considering the interaction between its transient current and transient voltage. Experimental results show that the proposed method can achieve  $10^5$ X speedup with an average accuracy loss of only 2.6% compared to the 3D mixed-mode TCAD simulation. Moreover, variation sources also become big issues with the progressing technology nodes and thus the proposed method is then extended to incorporate these variations during transient-fault analysis. As a result, sensitivity analysis that covers voltage, gate-length and device-width variations can be performed fast and accurately in our method.

## I. INTRODUCTION

The continued scaling of technology has produced more benefits for integrated circuit (IC) designs but has also degraded circuit reliability. The decrease in reliability can lead to system failures, and also creates more challenges when designing a robust system. Especially for safety applications (e.g., automotive, cloud, biomedical, military and etc.), achieving high reliability is always the first priority while performance is the second or after. Recently, soft errors have been emerged to be the dominant factor in the reliability degradation. A soft error is a transient fault induced by a radiation particle striking a device and later latched by a state-holding element. This type of errors will change the state of the design and may cause system failures.

There have been many research efforts investigating radiation-induced soft errors. In [1], the authors explored the charge collection mechanism and studied the impact of an angled ion strike using 3D technology computer aided design (TCAD) simulations. The authors in [2] measured the transient current in an nMOS/SOI transistor induced by heavy ions. The radiation effects for more advanced technological processes, such as FinFET and FDSOI, were presented in [3] and [4], respectively. However, all of the works mentioned above used TCAD simulation at the device level to meticulously analyze the radiation effect, resulting in prohibitively long computation time.

To design a robust system, it is important to mitigate soft errors in the early stages of the design flow to reduce cost. Therefore, an alternative fast soft-error-rate (SER) estimation

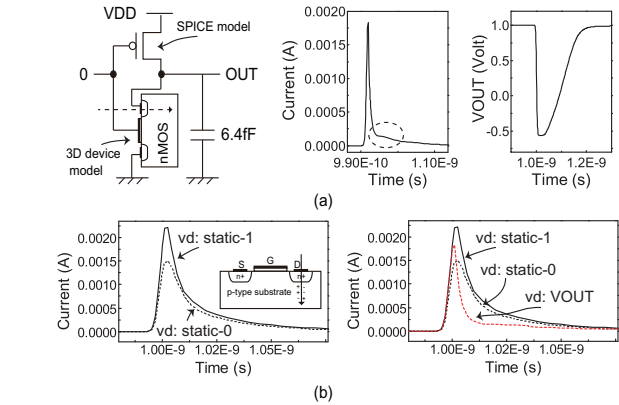


Fig. 1. (a) An example of the collected current and output voltage after a particle strikes the nMOS of the inverter. (b) Drain voltage impact on the collected current.

solution is desired, not an exhaustive TCAD simulation. Hence, an approximate exponential current source was first used in [5] to model the radiation-induced transient fault at the circuit level to improve efficiency of the SER analysis. This current source is injected into each cell of the design and then a SPICE simulation is performed to generate a transient voltage pulse. However, such approach is still time-consuming because it requires a large number of SPICE simulations for large circuit designs. Several approaches, later, were proposed to avoid the SPICE simulations by constructing look-up tables [6] or deriving analytic equations [7] based on the current source model. However, it is has yet to be determined whether this model is sufficient for accurately estimating radiation-induced transient faults in the era of more advanced technologies.

For example, consider the diagram in Fig. 1 (a). An inverter from the 45-nm technology node was implemented in a 3D mixed-mode simulation in which the nMOS (struck by a radiation particle) was modeled in the 3D device domain and the pMOS was modeled using a SPICE model. The results show that the collected current does not the exponential current waveform at all, which may result in an inaccurate estimation in advanced technologies. The same phenomenon is also noted in [8]. Another issue is that the current source model is a static model that is independent of the voltage of the sensitive node. However, different voltages in the sensitive node (i.e., the drain for the nMOS) produce electric fields with different strengths in the p-n junction and thus result

in different collected currents, as is shown in Fig. 1 (b). As a result, the collected current when the drain voltage is 0 v is entirely different from the current that is collected when the drain voltage is 1 v. In other words, the voltage of the sensitive node should be considered dynamically to ensure that the transient current estimation is accurate. In summary, the double-exponential current source may not be sufficient enough to describe radiation-induced transient faults in advanced technologies.

After understanding that the traditional double-exponential current model is no longer sufficient for advanced technologies, this work proposes a new fast-yet-accurate transient fault modelling method that can be used in the early stages of the design flow to reduce cost for the SER analysis. This modelling method, considering the interaction between the transient current and transient voltage, is done by a numerical method and a pre-built model that is assembled from a small number of device and circuit simulations to improve the accuracy of estimation. Note that the device and the circuit simulations are not required after the model is built. In recent years, the sources of variation, including process, voltage and temperature (PVT), have become a concerning issue with the advancing of the technology nodes. Hence, the proposed method also incorporates these sources to consider the variation effect and sensitivity of the transient-current estimation.

The remainder of this paper is organized as follows: Section II introduces the background of the radiation effect and the double-exponential current source model. The proposed fast-yet-accurate transient fault modelling method is elaborated in Section III. Experimental results on the model accuracy and variation analysis are presented in Section IV. Finally, Section V concludes this paper.

## II. BACKGROUND, REVIEW AND MOTIVATION

### A. Generation of Radiation-Induced Transient Faults

The physical mechanisms for the generation of a radiation-induced transient fault can be described in two steps: charge deposition and charge collection [9] [10]. Charge deposition is the phenomenon in which a particle releases a charge by direct or indirect ionization when it strikes a semiconductor device. In direct ionization, the particle generates electron-hole pairs along its trajectory and deposits the charge itself. Indirect ionization is when the incident particle does not directly release the charge itself. Instead, the incident particle interacts with the device, resulting in a nuclear reaction that produces secondary particles that deposit the charge. Heavy ions and alpha particles primarily deposit charge by direct ionization, and protons and neutrons tend to deposit their charge by indirect ionization.

After the charge is deposited, the deposited charge is collected by charge-collection mechanisms [9]–[11]. Consider the nMOS transistor as an example. In this transistor, the drain-bulk junction is a reverse-biased p/n junction with a strong electric field in the depletion region. When a particle enters the device, it collapses the original depletion region and

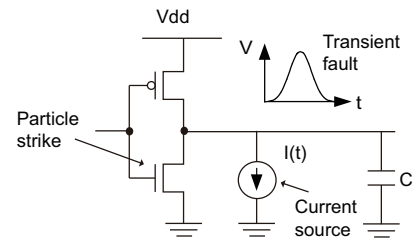


Fig. 2. Current source model of a particle strike at a circuit node.

distorts it along its trajectory, which has been referred to as a “funnelling effect” [11]. The deposited charge can be efficiently collected using the extending junction electric field and the drift process. Once the depletion region has recovered to its original width, the charge diffuses to the depletion region through the diffusion process. This collection mechanism is called the *drift-diffusion* collection mechanism. Both the drift process and the diffusion process exist in the heavily doped substrate, but there is only the drift process in the lightly doped substrate [12]. Note that there are also two other collection mechanisms—*bipolar effect* and *alpha-particle source-drain penetration (ALPEN)*—for collecting the deposited charge. More details about these two collection mechanisms can be found in [9], [10].

### B. Current Source Model

Traditionally, the radiation-induced transient fault is modeled as a double-exponential current source at the circuit level [5], [13]. This current source is injected into the output node of a cell in the design and is then simulated in SPICE to determine the radiation effect as shown in Fig. 2. The double-exponential current source can be described as follows:

$$I = \frac{Q_c}{\tau_\alpha - \tau_\beta} \times (e^{-\frac{t}{\tau_\alpha}} - e^{-\frac{t}{\tau_\beta}}) \quad (1)$$

where  $Q_c$  is the total amount of collected charge and  $\tau_\alpha$  and  $\tau_\beta$  are both process-related factors that correspond to the collection time constant and the ion track establishment constant, respectively.

Generally, the double-exponential pulse can describe transient faults accurately in older technologies (e.g., lightly doped substrate). However, the technology scaling has created several drawbacks to the model:

- 1) The collected current is not an exact exponential pulse as shown in Fig. 1 (a). As described in Sec. II-A, both drift and diffusion processes exist in heavily doped substrates (for advanced technologies), which results in the collection of more charge.
- 2) It is difficult to determine the global process-related factors,  $\tau_\alpha$  and  $\tau_\beta$ . The collected charge and  $\tau_\alpha$  and  $\tau_\beta$  will change based on different conditions such as the particle’s energy, position, etc. Determining global values for  $\tau_\alpha$  and  $\tau_\beta$  for accurately estimating the transient faults under different conditions is not easy to achieve.

3) The exponential model is a static model that is independent of the voltage of the sensitive node (i.e., the drain node of the nMOS). As described in Sec. II-A, the electric field of the p/n junction affects the efficiency of the charge collection procedure. For example, a higher drain voltage (i.e., stronger electric field) results in more collected charge as shown in Fig. 1 (b).

In summary, the double-exponential pulse is not sufficient to describe a radiation-induced transient fault. Another modelling method is necessary to ensure the accuracy and efficiency of the transient current analysis.

### III. PROPOSED TRANSIENT FAULT MODELLING METHOD

#### A. Proposed Method

As described in Sec. II, the transient voltage influences the collected currents according to the electric field of this transient voltage. This collected currents then charge/discharge the output loading and thus affect the transient voltage. Hence, for estimating the transient fault accurately, the interaction between transient current and transient voltage should be considered. The basic idea of proposed method is demonstrated in Fig 3. In this circuit, the cell is a simple inverter in which the input voltage is set to 0 v and the particle strikes in the drain of the nMOS. According to Kirchhoff's Current Law (KCL), the sum of all of the currents entering and exiting a node must equal zero. Hence, equations describing the current at node *out* of this inverter can be expressed as

$$I_p + I_c + I_s = 0 \quad (2)$$

$$I_s = I_n + I_{rad} \quad (3)$$

where  $I_p$  represents the drain current of the pMOS and  $I_s$  is the total drain current of the nMOS, including the drain current of the nMOS  $I_n$  and the radiation-induced transient current  $I_{rad}$ .  $I_c$  indicates the load capacitance charge current which is given by

$$I_c = C \frac{dV_{out}}{dt} \quad (4)$$

where  $C$  is the output loading of the inverter and  $V_{out}$  represents the voltage at node *out*.

Combining Eq. 2, Eq. 3 and Eq. 4, we have

$$I_p + I_n + I_{rad} + C \frac{dV_{out}}{dt} = 0 \quad (5)$$

We then apply the finite difference method to solve the differential equation (Eq. 5):

$$I_p + I_n + I_{rad} + C \frac{V_{out}^{i+1} - V_{out}^i}{t^{i+1} - t^i} = 0 \quad (6)$$

where  $t^{i+1} - t^i$  is a sufficiently small time step.  $I_p$  and  $I_n$  are both a function of  $V_{out}$ , and  $I_{rad}$  is dependent on both  $V_{out}$  and time. Because the built-in potential of a silicon diode is approximately 0.7 V, the maximum and minimum values of  $V_{out}$  are  $VDD + 0.7v$  and  $GND - 0.7v$ , respectively. Thus, we have

$$V_{out}^{i+1} = V_{out}^i - \frac{t^{i+1} - t^i}{C} (I_p(V_{out}^i) + I_n(V_{out}^i) + I_{rad}(V_{out}^i, t^i))$$

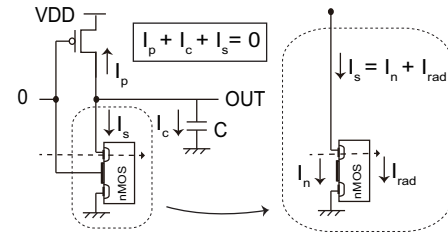


Fig. 3. The basic concept of radiation-induced transient fault modelling method. An example of inverter cell where nMOS is affected by the radiation particle.

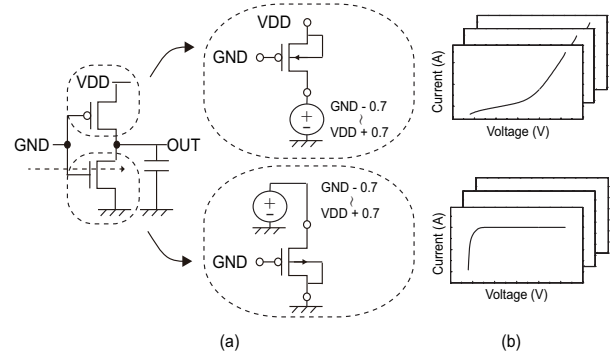


Fig. 4. (a) An example inverter used to precharacterize the current models,  $I_p$  and  $I_n$ , under various drain voltages. (b) The constructed I-V curve models.

$$V_{out}^{i+1} = \begin{cases} VDD + 0.7 & \text{if } V_{out}^{i+1} > VDD + 0.7 \\ GND - 0.7 & \text{if } V_{out}^{i+1} < GND - 0.7 \end{cases} \quad (7)$$

where the initial  $V_{out}^0$  is set to  $VDD$ . The models for currents  $I_p$ ,  $I_n$  and  $I_{rad}$ , will be described in next section. The process iterates until the output voltages are determined at each time point.

#### B. Pre-Characterization of the Current Models

To model the operating current and the transient current of the affected cell, an approach is proposed to extract the precharacterized models. The objective of these models is to estimate the currents at each time point and voltage conditions as described in Eq. 7. The models for radiation-independent currents  $I_p$  and  $I_n$  can be obtained from the SPICE simulation to avoid an exhaustive TCAD simulation. However, in order to consider the voltage and time dependencies of the transient current as described in Sec. II, a small number of meticulous TCAD simulation is performed to derive the model of the radiation-induced transient current ( $I_{rad}$ ).

Figure 4 contains a diagram of an example inverter that is used to precharacterize the current models for  $I_p$  and  $I_n$  via SPICE simulation. Because the particle strikes the nMOS of the inverter, a  $1 \rightarrow 0$  transient fault occurs and thus the input of the inverter should be set to 0 to activate the fault. Hence, both of the gates of nMOS and pMOS are connected to  $GND$  to characterize the models for  $I_n$  and  $I_p$ . Multiple DC analyses with different drain voltages are then repeated to compute the operating currents, as shown in Fig. 4. Fig. 4 (b) shows the re-

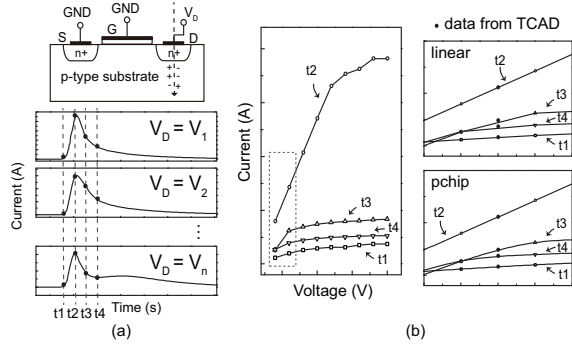


Fig. 5. (a) An example nMOS used to precharacterize the current models,  $I_{rad}$ , under various drain voltages. (b) Comparison of linear interpolation and pchip interpolation methods for estimating the transient current.

sulting I-V curve models, where the drain voltage ranges from  $GND - 0.7$  to  $VDD + 0.7$ . For a given voltage  $V$ , an efficient grid-based linear interpolation can be applied to estimate the current based on the constructed models. Note that, in this case, it is sufficient to only construct a one-dimension model to estimate the operating currents. However, the models may be extended to multiple dimensions to consider more complicated cases (i.e., variation-aware models).

The radiation-induced transient current model,  $I_{rad}$ , is also precharacterized in order to estimate the collected current once the particle strikes the sensitive region of device. The precharacterization for this current differs from the method used to construct the  $I_p$  and  $I_n$  models: the transient currents are measured using 3D TCAD simulations with various constant drain voltages as shown in Fig. 5 (a). Although the transient currents can be accurately calculated by 3D TCAD simulations, it requires a lengthy computation time to reflect the radiation effect. For example, it took over 5 hours to run a single case on our machine. For a given voltage  $V_d$  and time point  $t$ , the current can be interpolated from the precharacterized model. To avoid unnecessary simulations when characterizing the  $I_{rad}$  model, the piecewise cubic Hermite interpolating polynomial (pchip) interpolation method [14] is used instead of a linear interpolation method. As illustrated in Fig. 5 (b), if we apply the linear interpolation method to compute the current, the currents of the black points at time  $t3$  and  $t4$  cannot be accurately estimated and thus more data should be simulated to improve the accuracy. However, if we apply the pchip interpolation method, the currents can be computed correctly at any of the time points without additional data points.

### C. Variation Source and Internal Node Consideration

Radiation particles can not only affect output nodes but also internal nodes in a cell. An internal node strike is illustrated in Fig. 6, in which the particle strikes node  $n$  of a NAND cell and results in a transient fault. Similar to the concept described in Sec. III-A, the equation can be expressed as

$$I_{p1} + I_{p2} + I_s + C \frac{dV_{out}}{dt} = 0 \quad (8)$$

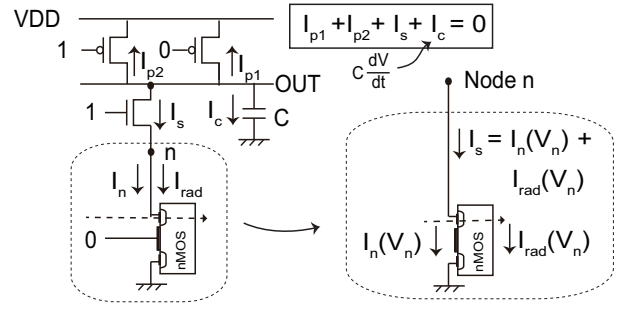


Fig. 6. An example of nand cell in which the internal node  $n$  is struck by a radiation particle.

This can be approximated as

$$V_{out}^{i+1} = V_{out}^i - \frac{t^{i+1} - t^i}{C} (I_{p1}(V_{out}^i) + I_{p2}(V_{out}^i) + I_s(V_{out}^i, V_n^i))$$

$$I_s(V_{out}^i, V_n^i) = I_n(V_n^i) + I_{rad}(V_n^i, t^i) \quad (9)$$

where  $V_n$  is the voltage of node  $n$  and can be computed by a root-finding algorithm.

With the continuous scaling of the technology, the PVT significantly influences not only the performance of the design but also the radiation effect estimation. As a result, the effects of variations are incorporated into the proposed modelling method to analyze the impact of variation and sensitivity on the transient current estimation. To consider the PVT effect, Eqs. 7 and 9 can be rewritten as

$$V_{out}^{i+1} = V_{out}^i - \frac{t^{i+1} - t^i}{C} (I_p(V_{out}^i, \vec{S}) + I_n(V_{out}^i, \vec{S}) + I_{rad}(V_{out}^i, t^i, \vec{S}))$$

$$V_{out}^{i+1} = V_{out}^i - \frac{t^{i+1} - t^i}{C} (I_{p1}(V_{out}^i, \vec{S}) + I_{p2}(V_{out}^i, \vec{S}) + I_n(V_n^i, \vec{S}) + I_{rad}(V_n^i, t^i, \vec{S})) \quad (10)$$

where  $\vec{S}$  is the set of desired variation sources. Current models that account for the variation sources can be constructed by the same method described in Sec. III-B. Note that some variations will not affect the collected current, and it is therefore unnecessary to characterize  $I_{rad}$  under those variations.

## IV. EXPERIMENTAL RESULTS

This section compares the accuracy between the proposed method and 3D TCAD simulations under different output loading conditions. A sensitivity analysis on the impact of the variations on the radiation effect estimation is then performed. The proposed framework was implemented in C++ and run on a Linux machine with a 16-core processor (2.4GHz) and 64GB of RAM. The technology used was the 45nm Nangate Open Cell Libraries [15].

### A. Accuracy of proposed method

In this section, the accuracy of the proposed method is demonstrated. For simplicity, the particle only strikes the nMOS transistor to verify the accuracy of the proposed

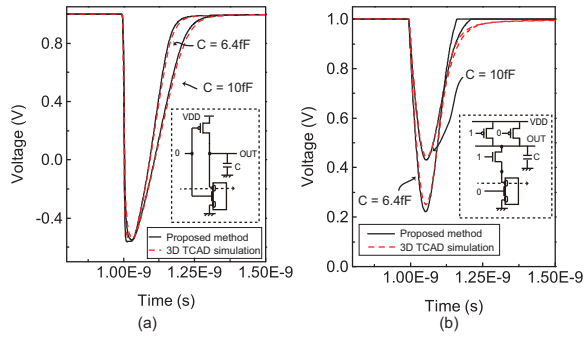


Fig. 7. (a) The output voltage of an inverter with output loadings of 6.4fF and 10fF. (b) The output voltage of a NAND cell after a particle strikes the internal node with output loadings are 6.4fF and 10fF.

method, and the linear energy transfer (LET) of the particle was prescribed as  $10 \text{ MeV} - \text{cm}^2/\text{mg}$ . Only 10 data points (one data point took  $\sim 5$  hrs to simulate) were needed to precharacterize the  $I_{rad}$  models when the pchip interpolation method was used to estimate the current.

Fig. 7 compares the output voltage from the proposed method and from the 3D mixed-mode TCAD simulation for an inverter and a NAND cell with two different output loadings, 6.4fF and 10fF. The black lines denote the results from the proposed method and the red dashed lines indicate the results obtained from the 3D mixed-mode TCAD simulation. The results show that the output voltage computed from the proposed method is very similar to the output voltage obtained from the 3D mixed-mode TCAD simulation, regardless of whether the particle strikes an output node (Fig. 7 (a)) or an internal node (Fig. 7 (b)). Table I summarizes the average errors between the proposed method and the TCAD simulation. The differences between the two methods for the inverter and the NAND cell are 2.5% and 2.7%, respectively. These results prove that the proposed method can accurately estimate a radiation-induced transient fault with an average error rate of only 2.6%.

Table I also lists the runtime of the proposed method and TCAD simulations. The runtimes of the 3D TCAD simulations for the inverter and the NAND cell were over 20 hrs. However, the runtimes for the proposed method for the inverter and the NAND cell were less 0.1s and 0.5s, respectively. Compared to the TCAD simulation, the proposed method significantly increased the speed of computation by about  $10^5$  on average. Moreover, the proposed method is also faster than the double-exponential current source approach. It is because that a SPICE simulation should be performed to transfer the double-exponential current source to transient fault voltage. Note that there are only two cells are performed in this study due to time limits. The radiation effects on the other cells can be analyzed based on the proposed method. In summary, the results demonstrate the accuracy and efficiency of the proposed method for the estimation of a radiation-induced transient fault. Thus, the method can be used for radiation hardening and variation sensitivity analyses.

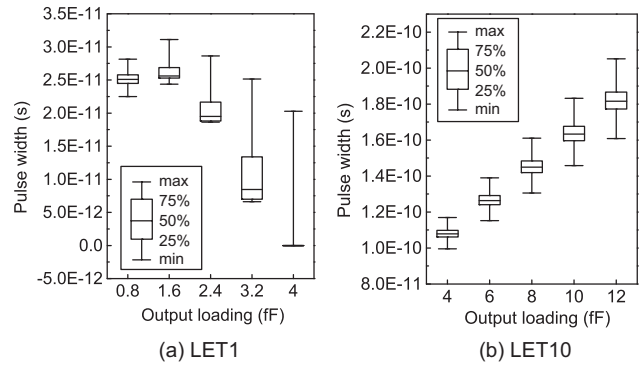


Fig. 8. Sensitivity analysis for 5% voltage variation for an inverter under five different output loadings and two different energy of particles: (a) LET1 and (b) LET10.

TABLE I  
ACCURACY AND EFFICIENCY OF PROPOSED METHOD AND 3D MIXED-MODE TCAD SIMULATION FOR SIMULATING A RADIATION-INDUCED TRANSIENT FAULT

Cell	Error	run time		Speedup
		Proposed method	TCAD simulation	
INV	2.5%	<0.1s	$\sim 27$ hrs	>972000X
NAND	2.7%	<0.5s	$\sim 20$ hrs	>144000X
average	2.6%	<0.3s	$\sim 23.5$ hrs	>558000X

### B. Variation sensitivity analysis

This section contains the sensitivity analysis for the process and voltage variations, where the process is varied by perturbing the gate width (W) and channel length (L) of the affected nMOS transistor. The pulse width of the radiation-induced transient voltage (50%-50% vdd), is used to measure the sensitivity of each variations, a common metric. Fig. 8 contains the sensitivity analysis for 5% voltage variations in a box-and-whisker plot for an inverter with two different energies, LET1 and LET10 and five different output loadings. The analysis yields the following two findings. (1) The voltage variation increases when the output loading increases under both energy conditions. Hence, one of the radiation hardening methods [16] that adds capacitive loads to mitigate the transient fault should be used carefully because the voltage variation may result in a larger variation of pulse width for the transient fault. (2) With the lower energy condition (LET1), the pulse width of the transient fault decreases as the output loading increases. This is due to the fact that the transient fault induced by a particle with low energy is weak (similar to Fig. 7 (b)), and it is therefore easy to be masked under large loading (most of the transient fault is masked since the output loading is 4fF). However, the pulse width increases because the output loading increases when the striking particle has a high energy (LET10). As shown in Fig. 7 (a), when a high-energy particle strikes, the drift process is very fast and a large amount of charge is left in the substrate that is then only collected by the diffusion process (very slow). It will take a longer time period for the pMOS to recover because a larger output loading of

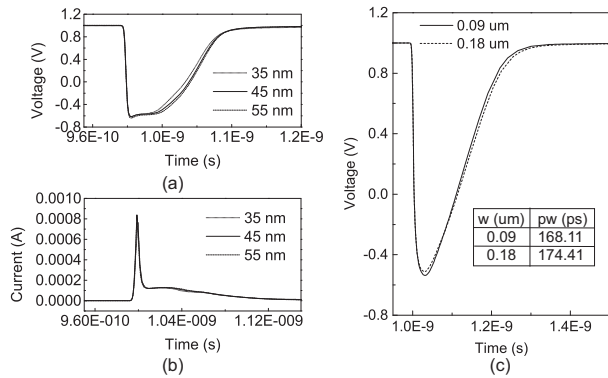


Fig. 9. Radiation-induced transient (a) voltages and (b) currents with three different gate lengths: 35 nm, 45 nm and 55 nm. (c) Radiation-induced transient voltages with two different device widths: 0.09 um and 0.18 um.

the inverter. This result supports the earlier conclusion that the designer should be careful to apply the added capacitance hardening method when a high energy particle strikes.

We next analyze the effect of variation in the gate length on the transient fault estimation. Fig. 9 (a) contains the radiation-induced transient voltages for a particle striking at nMOS of an inverter. In the example, the output loading is 1.6 fF, the energy of particle is LET10 and there are three different gate lengths: 35 nm, 45 nm, and 55 nm. It can be observed that a change in gate length does not result in a significant difference of the pulse width, as the pulse width variation is only 2% for a 10% gate length variation. This is due to the fact that the gate length fluctuation has only a small influence on the collected current (shown in Fig. 9 (b)). Additionally, because the nMOS is in the 'cut-off' state, the only change with the gate length perturbations is the leakage current.

Fig. 9 (c) illustrates the transient voltages induced by a particle striking an inverter, where the output loading is set to 10 fF and the energy of the particle is LET10. In this experiment, we fix the size of the pMOS (0.135 um) of the inverter but change the nMOS size to 0.09 um and 0.18 um, which produces transient voltage pulse widths of 168.11 ps and 174.41 ps, respectively. It can be observed that the larger device shows larger pulse widths, which is caused by the same phenomenon discussed above. Specifically, when the nMOS is in the 'cut-off' state, the increasing width only changes the leakage current, which is significantly smaller than the collected current. When a high-energy particle strikes, a larger-width device with a larger capacitance will have a longer recovery time. Note that the larger device width will result in a contradictory result when a low-energy particle strikes.

## V. CONCLUSION

With the continued scaling of technology, reliability (especially, soft errors) is now a critical issue to modern VLSI designs. To reduce cost in the early stages of the design flow, it is necessary to develop a method that can accurately and efficiently estimate transient faults. The traditional approach ignores effects in the advanced technologies and may no

longer provide sufficient accuracy for SER estimation. This study proposed a variation-aware transient current estimation method that considers the dynamic voltage based on pre-characterized current models and a numerical method. The benefits of the proposed method to estimate transient faults can be summarized as follows:

- 1) Any type of cells (sized cells and output loading) and any affected node of any cell (output and internal node) can be processed.
- 2) The proposed method is more efficient ( $10^5$ X speedup) than 3D mixed-mode TCAD simulation with an average loss of only 2.6%.
- 3) The variation and sensitivity analysis of the transient-fault estimation can be performed in an efficient manner.

## REFERENCES

- [1] P. Dodd, M. Shaneyfelt, and F. Sexton, "Charge collection and seu from angled ion strikes," *IEEE Transactions on Nuclear Science*, vol. 44, no. 6, pp. 2256–2265, Dec 1997.
- [2] T. Colladant, O. Flament, A. L'Hoir, V. Ferlet-Cavrois, C. D'hose, and J. du Port de Potcharra, "Study of transient current induced by heavy-ion in nmos/soi transistors," *IEEE Transactions on Nuclear Science*, vol. 49, no. 6, pp. 2957–2964, Dec 2002.
- [3] Y.-P. Fang and A. Oates, "Neutron-induced charge collection simulation of bulk finfet srams compared with conventional planar srams," *IEEE Transactions on Device and Materials Reliability*, vol. 11, no. 4, pp. 551–554, Dec 2011.
- [4] V. Malherbe, G. Gasiot, D. Soussan, A. Patris, J.-L. Autran, and P. Roche, "Alpha soft error rate of fdsoi 28 nm srams: Experimental testing and simulation analysis," in *IEEE International Reliability Physics Symposium (IRPS)*, April 2015, pp. SE.11.1–SE.11.6.
- [5] G. Messenger, "Collection of charge on junction nodes from ion tracks," *IEEE Transactions on Nuclear Science*, vol. 29, no. 6, pp. 2024–2031, Dec 1982.
- [6] A.-C. Chang, R.-M. Huang, and C.-P. Wen, "Casser: A closed-form analysis framework for statistical soft error rate," *IEEE Transactions on Very Large Scale Integration (VLSI) Systems*, vol. 21, no. 10, pp. 1837–1848, Oct 2013.
- [7] R. Garg, C. Nagpal, and S. Khatri, "A fast, analytical estimator for the seu-induced pulse width in combinational designs," in *Design Automation Conference*, June 2008, pp. 918–923.
- [8] R. Garg and S. Khatri, "3d simulation and analysis of the radiation tolerance of voltage scaled digital circuit," in *IEEE International Conference on Computer Design*, Oct 2009, pp. 498–504.
- [9] P. Dodd and L. Massengill, "Basic mechanisms and modeling of single-event upset in digital microelectronics," *IEEE Transactions on Nuclear Science*, vol. 50, no. 3, pp. 583–602, June 2003.
- [10] V. Ferlet-Cavrois, L. Massengill, and P. Gouker, "Single event transients in digital cmos - a review," *IEEE Transactions on Nuclear Science*, vol. 60, no. 3, pp. 1767–1790, June 2013.
- [11] C. Hsieh, P. Murley, and R. O'Brien, "Dynamics of charge collection from alpha-particle tracks in integrated circuits," in *Reliability Physics Symposium*, April 1981, pp. 38–42.
- [12] P. Dodd, F. Sexton, and P. Winokur, "Three-dimensional simulation of charge collection and multiple-bit upset in si devices," *IEEE Transactions on Nuclear Science*, vol. 41, no. 6, pp. 2005–2017, Dec 1994.
- [13] C. Zhao and S. Dey, "Modeling soft error effects considering process variations," in *International Conference on Computer Design*, Oct 2007, pp. 376–381.
- [14] F. N. Fritsch and R. E. Carlso., "Monotone piecewise cubic interpolation," *SIAM Journal Numerical Analysis*, vol. 17, pp. 238–246, 1980.
- [15] Nangate freepdk45 open cell library. [Online]. Available: <http://www.nangate.com/>
- [16] Y. Dhillon, A. Diril, A. Chatterjee, and A. Singh, "Analysis and optimization of nanometer cmos circuits for soft-error tolerance," *IEEE Transactions on Very Large Scale Integration (VLSI) Systems*, vol. 14, no. 5, pp. 514–524, May 2006.